

EXTENT AND EVALUATION OF LANDSLIDE PROBABILITY, TRIGGERING FACTORS AND MODEL VALIDATION IN SUB-HUMID AND SEISMICALLY ACTIVE AREA OF DISTRICT SHANGLA, EASTERN HINDUKUSH

SAJJAD MUHAMMAD KHAN^{1*} • ATTA-UR-REHMAN² • MUHAMMAD ALI¹

¹National Centre of Excellence in Geology, University of Peshawar, Peshawar, Pakistan.

²Department of Geography, University of Peshawar, Peshawar, Pakistan.

*Corresponding Author's Email: syed,sajjadmuhammad@uop.edu.pk

ABSTRACT

Alpuri valley is part of the Eastern Hindukush region of Northern Pakistan and is bounded by the lofty mountains. Geologically, it composes of the youngest mountain system and is mainly prone to frequently occurring landslides. Every year, human losses and damage to infrastructure are reported in the study area. The aim of this study is to prepare a comprehensive landslide inventory map and landslide susceptibility map using the Relative effect model. In order to achieve the objective, seventeen causative factors were selected on the basis of data availability. These factors are geology, slope, aspect, general curvature, profile curvature, plan curvature, topographic roughness index, drainage density, distance from road, distance from stream, NDVI, NDWI, stream power index, rainfall, land use land cover, distance from fault and elevation. The landslide inventory was prepared from the Google Earth and Sentinel 2 satellite images using the visual interpretation technique and field survey. A total number of 89 landslides were identified and mapped over the images. A bivariate statistical model i.e., Relative effect was used to evaluate the overall relationship between the causative factors and landslide occurrences and for the landslide susceptibility modelling. The developed landslide susceptibility map was classified into four classed very high, high, moderate and low categories, having 7.55% of the total area being very highly susceptible to the landslide and 27.31% of the total areas as low susceptible. The area under curve (AUC) method such as the success rate curve and prediction rate curve was used to verify the landslide susceptibility map. The prediction rate of the model was 87.87% to show the prediction power of the model whereas the success rate was 74.75% to show the accuracy of the susceptibility map. The landslide inventory and landslide susceptibility map can be helped for decision making and used for land use planning and landslide mitigation strategies.

KEYWORDS: landslide causative factors, Landslide susceptibility maps, Relative effect model, Alpuri valley

1. INTRODUCTION

Landslides are a recurrent and widely spread natural phenomenon all over the world (Dahal et al., 2008; Lv et al., 2022). The trend and frequency of

Extent And Evaluation of Landslide Probability, Triggering Factors and Model Validation in Sub-Humid and Seismically Active Area of District Shangla, Eastern Hindukush

Landslides are increasing day by day (Pareek et al., 2010; Rahman and Shaw, 2015). This severe hazard is especially found in the northern region of Pakistan which is covered with huge, lofty and rugged mountains (Khan et al, 2022). Pakistan consists of the three largest mountainous arcs such as Himalaya, Karakoram, and Hindukush (Baig et al., 2020; Rehman et al., 2022). Geologically these mountainous arcs are considered younger mountains system with weak and fragile slopes, fractured and folded and weathered rocks (Dahal and Hasegawa, 2008; Rehman et al., 2022). Various events such as landslides, glacial lake outburst floods, floods and earthquake activities (Rahaman and Shaw 2014; Rahman et al., 2019) are recurrent phenomena in the Hindukush-Himalayan region. Among them, landslides are the most terrible geological hazard in the Hindukush-Himalayan region of Northern Pakistan (Rahman et al., 2019). In the 2006 report of the P&D Department Shangla, the earthquake of October 8, 2005, caused life losses, damage to infrastructure and the economy. Earthquakes, flash floods, heavy rain and snow are the major natural hazards with high priority (<https://cms.ndma.gov.pk>). The frequently occurring phenomena found in these regions are the landslide which disturbs human life related to their activities (Crozier, 1986; Kamp et al., 2009). Most of the research find out that one-third of landslides are present in the Himalayas region of the world (GOP, 1987; Khan, 2000). This problem represents small-scale to large-scale landsliding and depends on the topographic, morphologic, hydrologic and climate change factors (Groneng et al., 2011; Vandromme et al., 2020). Kashmir is an example of a landslide-prone area in the Himalayan region (Khattak et al., 2010; Zaz and Romshoo, 2022).

Alpuri valley is part of the eastern Hindukush mountain region which is vulnerable to landslide hazards. Alpuri valley is bounded by lofty mountains and is considered a severe landside area. Earthquakes and heavy rain are the major causes to generate the landslides in the study area. heavy rains during Monsoon Season from July to September are prone to landslides. In this study, landslide susceptibility mapping of Alpuri valley was generated by using the landslide causative factors with past landslides to analyze the landslide probabilities and help the planner for future planning and management. The landslide causative factors were related to geological, hydrological, topographic and other related factors.

Various types of models have been prepared for landslide susceptibility assessment (Luo and Liu, 2018). These models are based on a qualitative and quantitative approach. Qualitative models are subjective, based on experts' experiences and opinions are very important role (Ada and San,

2018; Feizizadeh et al., 2014; Hong et al., 2017b; Pourghasemi et al., 2012). These are such as geomorphological mapping (Reichenbach et al., 2005), heuristic or index-based method (Ercanoglu and Gokceoglu, 2002; Pourghasemi et al., 2012), and analysis of landslide inventory (Galli et al., 2008). Quantitative methods are objective, based on the mathematical/statistical equations which analyze the relationship between the landslide base environmental factors and past landslides (Arnone et al., 2016; Sezer et al., 2017), frequency ratio (FR) (Wang and Li, 2017; Khan et al. 2019), logistic regression, naive Bayes (Pham et al., 2017a), weight of evidence (Ilia and Tsangaratos, 2016; Razavizadeh et al. 2017) etc., are quantitative-based methods.

To solve this problem, Relative Effect is one of the quantitative base model, utilized for landslide susceptibility assessment in Alpuri Valley. this approach has been used by various researchers to identify the landslide susceptibility assessment in hilly areas (Ghafoori et al., 2006; Naveen Raj et al., 2011; Neelakantan and Yuvaraj, 2012; Pradhan and Kim, 2014; Ramesh and Anbazhagan, 2015). Relative effect model can be better used for constitution, investigation and identification of landslides. The past landslide inventory map was developed and combined with causative factors with the help of Relative Effect model to find out the landslide possibilities area in Alpuri valley. Area under the curve (AUC) was used to indicate the performance and accuracy of the model.

2. MATERIAL AND METHOD

Alpuri valley is a part of the Shangla District and has been considered in the present research study (Fig 1). Location coordinates of Alpuri valley are 34.94N and 72.65E (WGS). Approximately, it covers an 812Km² area of Shangla District. Topographically, the area is surrounded by high and rugged mountains. Its elevation from sea level is 1471 meters. Climatically, Alpuri Valley is temperate and warm. In Alpuri Valley, 15.8°C and 1010mm are the average annual temperature and rainfall. 623.7 Km² is the density of population in Alpuri Valley. This area is considered a landslide-prone area in Northern Pakistan. It causes the loss of human lives and damaged infrastructure.

The objective of the research is to use the geospatial techniques along with the various software to prepare the landslide susceptibility map. In the present research, 17 landslide causative factors such as elevation, slope, aspect, general curvature, profile curvature, plan curvature, stream power index, drainage density, terrain roughness index, normalized difference vegetation index (NDVI), normalized difference wetness index (NDWI), geology, distance from stream, distance from road, distance from

Extent And Evaluation of Landslide Probability, Triggering Factors and Model Validation in Sub-Humid and Seismically Active Area of District Shangla, Eastern Hindukush

fault, Landuse Landcover and rainfall data were highlighted for the responsible in triggering the landslides and selected for landslide susceptibility mapping (Table1). In the beginning, the landslide inventory map was prepared with the help of fieldwork, Google Earth and sentinel images of the study area. A total of 89 landslides were mapped in the landslide inventory map.

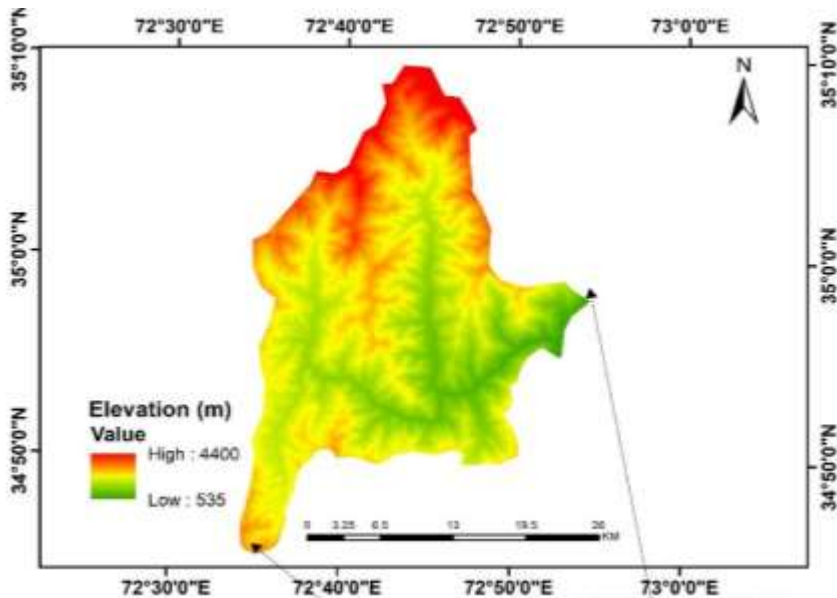


Fig. 1. Alपुरi Valley

The ALOSPALSAR DEM (12.5 m resolution) was used to extract the morphometric terrain attributes such as slope, aspect, general curvature, profile curvature, plan curvature, terrain roughness index, stream power index, drainage density, and elevation. Sentinel satellite images (10m resolution) of the study area were downloaded from the website. These images were used to develop the normalized difference vegetation index (NDVI), and normalized difference wetness index (NDWI). Sentinel Satellite Landuse Landcover images having 10m spatial resolution were used to extract the landuse landcover causative factor. Faults were digitized from the fault map of Besham. The geology map was digitized from the geological map of north Pakistan. Distance from the road, distance from Stream and distance from faults were created from multiple buffer tools in ArcGIS software. Rainfall data was downloaded from Global Precipitation Measurement Mission and converted into point data. The IDW interpolation technique was used to generate the rainfall map. All vector data was converted into raster data in Arc GIS for analytical purposes. The process of landslide susceptibility mapping was divided into three sections.

In the first section, digitized landslide inventory map and selection of causative factors. In the second section, Relative Effect model the logarithmic model was used to find out the correlation of landslide inventory with the selected causative factors. The inventory map was set into test and training data set and prepared the landslide susceptibility map. In the third section, the validation and performance of the selected model were checked by using the testing and training data set. AUC was used to calculate the success and predictive curve rates. Success curve rate was used for overall data whereas, predictive curve rate was used for validation purposes. All the landslide thematic maps were integrated into the GIS environment.

Relative Effect model (Pradhan and Kim, 2014; Ramesh and Anbazhagan, 2015) was calculated by using the equation given below;

$$RE = \text{Log} \left(\frac{SR}{AR} + \varepsilon \right) \quad (1)$$

Whereas,

$$SR = \frac{sld}{SLD} \quad (2)$$

$$AR = \frac{a}{A} \quad (3)$$

Whereas relative effect shows as RE, **a** indicates the area of each class in an individual class, **A** is the total area of the study area, **sld** represents the total area of landslide in an individual class, **SLD** is a total area of landslide in the study area., ε is the small positive value near to zero. The value of Relative Effect model was calculated for all classes of 17 selected causative factors (Table 1).

A positive value represents the strong relationship between the landslide occurrence and classes of each factor map. Landslide susceptibility is high in positive value. But negative value indicates weak relation between each class of factor map with landslide occurrence and low landslide susceptibility. In case of zero value, no relationship is found between the landslide occurrence and causative factor. All the factor maps were integrated into the GIS environment to calculate the landslide susceptibility index by using the Relative effect values using equation 9. The resultant map known as landslide susceptibility mapping was developed from the landslide susceptibility index and classified into four zones.

3. RESULT AND DISCUSSION

Landslide is a natural hazard in northern Pakistan. Due to landslide hazards, multiple cases were reported throughout the years in Pakistan. Downward movement of the mass of debris, earth, or rocks under the effect of gravity is known as landslides (Cruden, 1991). Geological causes, the intensity of rainfall and earthquake are the trigger factors of landslide events (Lee and Talib, 2005). It causes losses in terms of properties and human life as well as resources (Davies, 2015). Landslide is not a new thing and its mitigation is necessary to prevent it in future. Mapping of landslide affected area is very important to determine the susceptibility zones of landslide. Relative effect is one of the popular model of landslide susceptibility mapping.

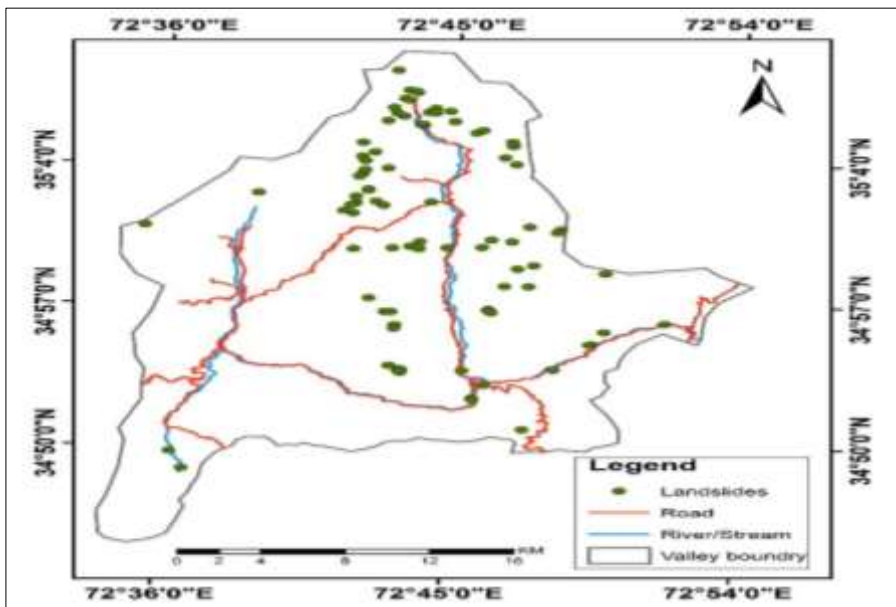


Fig 2. Alपुरi valley, landslide inventory and distribution of past landslides.

3.1 Preparation of landslide inventory

In the statistical analysis of Landslide susceptibility, landslide inventory plays a significant role to extract the information on parameters of the landslide affected and adjacent areas (Bui et al., 2011; Shit et al., 2016). Landslide inventory provides information on landslide distribution (Mondal and Mandal, 2017). The landslide inventory indicates the area, location, shape, and types of movements and materials of the landslide area. GPS was used in the field survey to conduct landslide information (Bai et al., 2010). Satellite images and google earth were the other resources to

collect landslide information. Total of 89 landslides was digitized and rasterized into the 12.5 by 12.5m spatial resolution. Fig 2 is showing the spatial distribution of landslides. This was used to calculate the ratio of landslide frequency with the help of several cells in a different class of selected factors.

Table 1. Landslide causative factors and their Relative effect values to landslide.

Causative Factors	Classes	% Of total Pixels in Class	% Of Landslide Pixels in Class	Relative effect value
Geology	Kamila Amphibolites (Ka)	25.14	30.01	0.08
	Indus Suture Melange (Ism)	20.07	22.19	0.04
	Swat Granites (Swg)	2.58	0.14	-1.26
	Cambrian Manglaur (Cb)	2.52	2.84	0.05
	Karora group (Pr)	18.13	8.82	-0.31
	Besham formation (A)	20.00	28.59	0.16
	Alpuri group (Ms)	11.56	7.40	-0.19
Slope Gradient	0 - 18	11.31	9.06	-0.096
	18 - 28	23.47	18.97	-0.093
	28 - 36	30.89	33.29	0.032
	36 - 46	24.99	27.88	0.047
	46 - 78	9.34	10.81	0.064
Slope Aspect	North	10.24	8.38	-0.17
	Northeast	11.05	13.44	0.09
	East	14.45	19.03	0.12
	Southeast	15.84	18.84	0.08
	South	12.23	16.14	0.12
	Southwest	13.05	9.42	-0.14
	West	12.38	7.86	-0.20
Distance From Road	0 - 200	8.22	20.63	0.40
	200 - 400	7.06	7.40	0.02
	400 - 600	6.52	3.18	-0.31
	600 - 800	6.13	2.09	-0.47
	>800	72.07	66.71	-0.03
Distance From stream	0 - 200	5.17	20.72	0.60

Extent And Evaluation of Landslide Probability, Triggering Factors and Model Validation in Sub-Humid and Seismically Active Area of District Shangla, Eastern Hindukush

	200 - 400	5.00	3.41	-0.17
	400 - 600	4.89	5.97	0.09
	600 - 800	4.79	2.89	-0.22
	>800	80.16	67.00	-0.08
General Curvature	-73.60 - -4.96	2.02	2.18	0.03
	-4.96 - -1.77	17.61	23.47	0.12
	-1.77 - 0.89	50.30	51.45	0.01
	0.89 - 4.61	28.07	20.39	-0.14
	4.61 - 6.08	2.00	2.51	0.10
Elevation	535 - 1459	15.42	21.57	0.15
	1459 - 1973	30.07	22.90	-0.12
	1973 - 2482	30.96	29.45	-0.02
	2482 - 3158	16.00	25.65	0.21
	3158 - 4400	7.56	0.43	-1.25
Plan Curvature	-32 - 2.06	4.23	5.17	0.09
	-2.06 - -0.70	20.02	24.56	0.09
	-0.70 - 0.39	39.77	41.01	0.01
	0.39 - 1.75	29.19	23.38	-0.10
	1.75 - 37.40	6.80	5.88	-0.06
Profile Curvature	-25.84 - -2.57	3.10	3.18	0.01
	-2.57 - -0.72	21.82	16.64	-0.12
	-0.72 - 0.60	44.82	43.24	-0.02
	0.60 - 2.45	26.52	32.48	0.09
	2.45 - 41.60	3.74	4.46	0.08
Terrain Roughness Index	0.10 - 0.38	6.62	13.04	0.29
	0.38 - 0.46	22.13	22.76	0.01
	0.46 - 0.52	35.74	42.58	0.08
	0.52 - 0.59	26.60	16.17	-0.22
	0.59 - 0.95	8.91	5.45	-0.21
NDVI	-0.40 - 0.18	2.63	11.66	0.65
	0.18 - 0.39	7.10	44.71	0.80
	0.39 - 0.53	18.84	24.23	0.11
	0.53 - -0.62	35.38	13.13	-0.43
	0.62 - 0.86	36.04	6.26	-0.76
Stream Index	Power 0 - 17346033	99.93	99.53	0.00
	17346033 - 69384135	- 0.05	0.33	0.81
	69384135 - 160450813	- 0.01	0.14	0.99
	160450813 - 307892102	- 0.00	0	0

	307892102	- 0.00	0	0
	55904832			
NDWI	-0.74 - -0.52	26.57	4.98	-0.73
	-0.52 - -0.44	38.76	14.46	-0.43
	-0.44 - - 0.33	23.11	27.50	0.08
	-0.33 - 0.17	8.37	41.68	0.70
	0.17 - 0.51	3.19	11.38	0.55
Drainage Density	0 - 0.56	81.57	68.14	-0.08
	0.56 - 1.12	8.73	10.05	0.06
	1.12 - 1.68	7.20	7.11	-0.01
	1.68 - 2.24	2.13	8.20	0.59
	2.24 - 2.8	0.36	6.50	1.26
Landuse Landcover	Bare Land	0.75	1.70	0.38
	Built Area	18.98	18.96	0
	Clouds	0.00	0	0
	Crops	0.27	0	0
	Rangeland	37.74	59.69	0.20
	Snow/Ice	2.68	0	0
	Trees	39.35	18.72	-0.32
Distance Fault	From 0 - 200	11.57	17.21	0.17
	200 - 400	10.93	13.94	0.10
	400 - 600	10.14	9.01	-0.05
	600 - 800	9.23	8.25	-0.05
	>800	58.13	51.59	-0.05
Rainfall	96.73 - 101.88	10.21	16.83	0.22
	101.89 - 105.67	18.74	24.37	0.11
	105.68 - 109.21	26.96	26.22	-0.01
	109.22 - 112.43	25.45	20.19	-0.10
	112.44 - 117.26	18.61	12.37	-0.18

3.2 Relationship between causative factors and Relative effect model

3.2.1 Surface geology and relative effect model

The geology and tectonics of the Northern Pakistan region is evidence of the collision of the Indian and Eurasian plate. Tectonic movements and lithology units have a great effect on slope instability because of their different susceptibilities (Dai et al., 2002; García-Rodríguez et al., 2008; Nefeslioglu et al., 2008). The geology map of the study area was prepared from the geological map of northern Pakistan (Fig 3a). Fig 4a; Table 1 is showing an overall correlation between geology and landslides and relative effect values. Relative effect values of lithological units such as

Extent And Evaluation of Landslide Probability, Triggering Factors and Model Validation in Sub-Humid and Seismically Active Area of District Shangla, Eastern Hindukush

Besham formation, Indus suture melange, Cambrian Manglaur, and Kamila Amphibolites were high which indicated a high possibility of landslides occurrence. Besham group appeared in the Late Archean to Early Proterozoic. This group is sub-grouped into Thakot and Pazang formations. This formation is based on less quantity of calcareous, graphitic schist gneiss, marbles, psammite, and banded quartzite. Manglaur formation contains quartz, quartz-mica-garnet schist, and graphitic schist. Indus suture mélangé which consists of serpentinite, melanges and high-pressure blueschists. Kamila Amphibolite belt is meta plutonic rock. Khan et al. (1997) determined the Kamila Amphibolite belt as a complex mass of amphibolite facies meta plutonic and metavolcanic rocks. According to Rahman et al., (2019), it is identified that Besham group showed high susceptibility score, Cambrian Manglaur showed second high susceptibility score whereas, Karora group has the lowest susceptibility score by using the frequency ratio model. In this research, the same result was found. Besham group show a strong correlation with landslide events whereas Karora group shows weak relation with landslide events. Other lithological units such as Kamila Amphibolites and Indus Suture Melange also have a positive impact on landslide possibilities.

3.2.2 Slope gradient and Relative effect model

Slope gradient is a direct effect and triggering factor on landslide occurrence (Lee and Min, 2001). Landslide events depend on the slope angle which affects the surface runoff, shear stress on the slope and weather process (Meena and Gudiyangada Nachappa, 2019). The angle of slope increases then the shear force also increases which will induce the landslides (Pham et al., 2017c). It increases the density ratio of landslides with an increase in the slope gradient (Dai et al., 2001; Rahman et al., 2017). Slope gradient was extracted from the ALOSPALSAR DEM having 12.5m resolution (Fig 3b). Slope gradient was classified into five classes by using the natural break. As a result, relative effect value for each class of causative factors was calculated and shown in Fig 4b; Table 1. The analysis revealed that a high frequency of landslides has been found from 28 degrees to 78 degrees of slope which indicated a strong correlation with landslide events. It was found that anthropogenic activities are high which increases the ratio of landslides.

3.2.3 Slope aspect and relative effect model

Orientation of slope is called slope aspect which consists of 9 directions of slope (Bui et al., 2014; Pham et al., 2018). The relation of slope aspect is indirect with landslide occurrence. Slope aspect depends on the duration

and intensity of solar radiation, vegetation type, evapo-transportation and precipitation (Kouli et al. 2010; Shirzadi et al., 2017). The slope aspect factor was extracted from ALOSPALSAR DEM as shown in Fig 3c. In this study, northeast to south-facing slopes have high intensity of solar radiation and precipitation both during winter and monsoon seasons. Highest values of the slope aspect were indicated in the east and south direction which described strong relation and high possibility of landslide occurrence in the study area as shown in Fig 4c; Table 1. This result indicated the same result of Rehman et al. (2019) in the Shahpur Valley, Shangla district. Other active phenomena such as thermal expansion and contraction are exposed to the sunlight on the south-facing slope. East-facing slopes have contact with high rainfall in the monsoon season. This analysis showed that variation of intensity of rainfall and duration and intensity of solar radiation has a relationship with the variation in density of landslide occurrence.

3.2.4 Elevation and relative effect model

Elevation is related to the topographic causative factor (Table 1). It affects various geologic and geomorphic conditions. It classified the relief based on maximum and minimum elevation above the sea level (Youssef et al., 2014). It plays the role of an indicator of landslide and predictive factor for landslide susceptibility mapping. Elevation factor was extracted from ALOSPALSAR DEM as shown in Fig 3d. It is classified into five classes. Table 1; Fig 4d showed the highest relative effect value of class (2482 - 3158) has highest positive relative effect value of 0.21, indicating the high tendency of landslide occurrence as compared to the other classes. The second-highest relative effect value was found from 535 to 1459 m elevation. Most of the population and infrastructure are found in these classes. Infrastructure development decreases the vegetation-covered area and cuts the toe of the slopes which increases the rate of landslides in the study area.

3.2.5 Distance from stream and relative effect model

River works as an agent of erosion. Fluvial cycle is an example of an erosion process where subsurface and surface flow water eroded the base of slope. These erosion activities take place near the river. The area where the river density is high indicated the area has high susceptibility to landslide events (Hong et al., 2015; Myronidis et al., 2015; Chen et al., 2016). Regular flow of water in a river can destroy the strength for slope declination which generate the landslides surrounding the river. Proximity of rivers is determined by distance from stream. In Alpuri Valley, the distance from stream map was developed through multiple buffers around

the streams as shown in Fig 3e. Multiple buffers were generated at 200m intervals with the help of the multiple buffer tool in ArcGIS. The resultant value of relative effect indicated that high value was calculated near the river which represents high possibility of landslide occurrence due to high runoff water and lateral erosion process in stream, especially during the summer monsoon as shown in Fig 4e; Table 1. In the study of Rehman et al. (2019), the same result was found that susceptibility was high near the river and low when moving away from the stream.

3.2.6 Distance from road and relative effect value

Road is an androgenic agent, that takes part in landslides in hilly areas (Jaafari et al., 2014; Zhao et al., 2015). Road construction and expansion are the factors which support the erosion process and disturb the continuity of rocks and soil masses and destabilize the slope. In this research, the distance from road factor was generated with the help of buffers around the road as shown in Fig 3f. 200m interval has been placed between every buffer zone. Value of every class of factor was measured through relative effect model which determined the influence of landslide occurrence. The resultant value indicates that near to road has a high possibility of landslide events due to erosion process, road construction, vehicle movement, and road expansion. This possibility decreases when moving away from the road (Fig 4f; Table 1). In the analysis of Rehman et al. (2019), the landslide susceptibility score was high near to road and decreased when moving away from the road.

3.2.7 Stream power index and relative effect model

Stream power index is the hydrological factor which is utilized to calculate the erosion power of the water inflow accumulation area (Moore and Wilson, 1992; Mohammady et al., 2012; Sun et al., 2018). It shows the direct relation of erosion power with slope toe erosion (Nefeslioglu et al., 2008). The stream power index is a quantitative value based on a hypothesis (Moore et al., 1991). The equation of stream power index is given below;

$$SPI = A \frac{\tan\beta}{b} \quad (4)$$

Whereas,

A is the flow accumulation area and b is slope gradient. In Alpuri valley, the relative effect model is used to calculate the value of Stream power index. The stream power index was classified into five classes as shown in Fig 3g.

As a result, the relative effect values were calculated for the entire Alpuri Valley and visualized and tabulated in Fig 4g; Table 1. It was found from the analysis that Second and Third class of SPI shows a positive correlation with relative effect values of 0.81 and 0.99 respectively which indicated the high ratio of erosion power of water and possibility of landslide occurrences.

3.2.8 Drainage density and relative effect model

Drainage density is an indirect factor of landslide events. It describes the lithology, climate, relief, structure landform flux density and vegetation of the study area (Udin et al., 2021). Runoff water from streams is important for drainage density. Runoff water carries the eroded material in a hilly area and causes the landslide (Mitra et al., 2017). The drainage density can be calculated by dividing the total length of the stream by the total area of a drainage basin. The drainage density can be calculated as:

$$DD = \left(\frac{LS}{AD} \right) \quad (5)$$

Whereas,

Drainage density represents by DD, LK is the total length of steam/ river and AD is the total drainage basin area of the study area. Drainage density is the quantitative value defined from low to high. High value represents the high ratio of runoff and low rate of infiltration. Due to the high velocity of water flow and low infiltration rate, the possibility of landslide occurrence increases. In this study, drainage density map was prepared in a GIS environment as shown in Fig 3h. Map classified into five classes. Each class was calculated the relative effect value, which indicated the influence of the landslide event (Table 1). The result showed that value increases from low density to high drainage density. It is also observed that drainage density from 1.68 to 2.8 showed high relative effect value than other classes. So the rate of landslide events is high tendency in this range of drainage density. The overall result of each class of factors is shown in Table 1; Fig 4h.

3.2.9 Normalized difference Vegetation index and Relative effect model

Normalized Difference Vegetation Index is causative factor of landslide occurrence (Lundgren, 1972). This index represents the density of vegetation in the study region (Iqbal et al., 2021). Forest, crops, rangeland etc. on the land surface are the different forms of vegetation (Guo et al., 2015; Eker et al., 2015; Chen et al., 2016). It gets negative impact on

landslide occurrences when the presence of dense vegetation and positive in the absence of vegetation. Dense vegetation decreases the erosion process and increases the cohesion strength in soil. The normalized vegetation index was calculated from the difference between an infrared and red band of satellite images. Calculation of index is given by (Justice et al., 1985):

$$NDVI = \frac{NIR - RED}{NIR + RED} \quad (6)$$

Whereas NDVI is the normalized difference vegetation index, NIR is infrared wavelength band of satellite image. RED is the red wavelength band of satellite images. The index value was found between -1 and +1 value. -1 value indicates less vegetation area and +1 indicated dense vegetation area. In Alpuri Valley, NDVI map is classified into five classes which define the concentration of vegetation in each class (Fig 3i). The relative effect value was calculated which defines the frequency of landslide occurrence in each class. On basis of relative effect values, the NDVI class of 0.18-0.39 is showing highest value to determine the high possibility of the landslide which shows a positive correlation between the causative factor and landslides. whereas, NDVI class of 0.62 – 0.86 has less prone to landslide occurrences (Table 1; Fig 4i).

3.2.10 Normalized difference water index and relative effect

Normalized difference water index was developed by McFeeters (McFeeters, 1996). This index gives the knowledge about the water bodies in the study area as shown in Fig 3j. It is used to find out the soil depth, erosion rate, and wetness (Aslam et al., 2021). Satellite image was used to calculate the normalized difference water index by utilizing the green band and the Near-infrared band of the satellite image. Following equation used to measure the NDWI is given below:

$$NDWI = \frac{(BAND\ GREEN - BAND\ NIR)}{(BAND\ GREEN + BAND\ NIR)} \quad (7)$$

NDWI has values which define the ratio of water bodies on the surface. If the value is less than zero it represents the no water body present on the surface area whereas if the value is greater than zero identified the water bodies on the surface area. The relative effect value for each class of NDWI was calculated which indicated the presence or absence of water bodies by increasing or decreasing the values. when analysing the result of NDWI, the relative effect values were increased toward NDWI class of (0.17 – 0.51). The NDWI class of (-0.33 – 0.17) indicated high relative effect value

which revealed high frequency of landslides and high susceptibility to landslide events (Fig 4j; Table 1).

3.2.11 Terrain Roughness index and relative effect

Terrain roughness index plays a positive role in landslide occurrence (Jebur et al., 2015). Terrain term was used for the local relief in the study. Terrain roughness index is the index to find out the ruggedness of the terrain (Al-Najjar and Pradhan, 2021). Range value describes the heterogeneous situation of the local terrain. Terrain roughness index is the following formulation:

$$TRI = \sqrt{|x|(max^2 - min^2)} \quad (8)$$

Whereas,

max represents steep slope and roughness of the terrain surface and min represents the flat and smoothness of surface terrain (Riley et al., 1999). Range of data present from 0 to 1.

High roughness of surface terrain indicates high heterogeneity and low roughness shows the smoothness or homogeneity of the landscape. Raster calculator tool was used to calculate the terrain roughness index as shown in Fig 3k. Relative effect value of each class was calculated to identify the impact of landslide events. It was identified that first class was high value of relative effect model which shows high rate of landslide occurrence (Fig 4k; Table 1). It is observed that positive values of TRI show smooth to low ruggedness of the landscape which represents a strong correlation between landslides and causative factors and is highly prone to landslide occurrences.

4.2.12 General curvature and relative effect model

Curvature is the topographic factor which helps in the landslide hazard analysis. Mathematically, it is a change in slope gradient with respect to a very small arc of curve (Thomas, 1968). It works opposite the radius of circle in form of a tangent over a small arc (Kepr, 1969). The curvature line formed at the intersected point of imaginary plane with ground surface. In landslide analysis, three values of curvatures were used (Dikau, 1989; Moore et al., 1993a, b; Ayalew and Yamagishi, 2004). The curvature is divided into classes such as concave, convex, and neutral. The neutral class is the flat area and has zero value. The concave class consists of positive and concave class indicates negative value. ALOSPALSAR DEM was used to extract the general curvature (Fig 3l). Relative effect values of each class were calculated to find out the influence of landslide occurrence. In this

Extent And Evaluation of Landslide Probability, Triggering Factors and Model Validation in Sub-Humid and Seismically Active Area of District Shangla, Eastern Hindukush

study area, general curvature class from -73.60 to -1.77 showed the concave class with the relative effect value of 0.30 and 0.12, respectively. Class from -1.77 to 0.89 represents the flat class with a value of 0.01 and class from 4.61 to 6.08 shows the convex class with a value of 0.10. All these classes determine positive relation between landslide and high influence and susceptible to landslide events (Fig 4l; Table 1).

3.2.13 Profile curvature and relative effect model

Profile curvature is downward in slope direction to indicate the movement of sediment and erosion (Chen and Chen, 2021). It works to control the runoff of the water (Pourghasemi et al., 2018). It is a curvature line prepared by the intersection of a vertical plane with ground surface (Al-Najjar and Pradhan, 2021). Generally, it is classified into three areas such as convex, concave, and flat or neutral. It is the inverse of plan curvature. Convex surface contains the positive profile curvature and concave surface consists of negative profile curvature. It influences the resisting and driving pressure in the landslide movement within the landslide. ALOSPALSAR DEM was utilized to develop the profile curvature as shown in Fig 3m, and relative effect model was used to measure the values of each class of factor. As a result, it is observed that concave surface identified a high ratio of landslides and strong relationship with the landslide events as compared to the convex and flat surface (Fig 4m; Table 1).

3.2.14 Plan curvature and relative effect model

Plan curvature is the inverse of profile curvature where it is prepared by the intersection of imaginary horizontal plane with ground surface (Kannan et al., 2013; Iqbal et al., 2021). Plan curvature determines the convergence and divergence of landslide material and the flow of water in the landslide movement path (Carson and Kirkby, 1972; Yilmaz et al., 2012). Concave, convex and flat is a subdivision of plan curvature. Concave is the convergent part having positive value, convex is the divergent part, having negative value and flat is the neutral part, having zero value. ALOSPALSAR DEM was employed to prepare the plan curvature factor and five classes were generated as shown in Fig 3n. Relative effect model was used to find out the relative effect value of each class to determine the influence of landslide events in each class of the factor. As a result, the positive correlation and high concentration of landslide events for concave class as compared to flat and convex classes as shown in Fig 4n; Table 1.

3.2.15 land-use land-cover and relative effect model

Land use landcover is an anthropogenic and affected factor in most landslide susceptibility studies. Land use of any area is affected by human intervention and infrastructure development. Several publications have considered landuse landcover factors in their analysis (Restrepo et al. 2003). However, vegetative cover area has low erosional activity as compared to bare area having unconsolidated material. In this study, Sentinel 2 landuse landcover classified satellite images having the 10m spatial resolution were used to extract the landuse landcover map of the study area (Fig 3o). As a result, Fig 4o; Table 1 shows that the highest relative effect value was found in Bare land-use class. The bare land is showing the value of 0.38 and indicates a positive relation with landslide events. The second highest value was found in the Rangeland class and showed the value of 0.20. rangeland also shows high susceptibility to landslides. The analysis revealed that bare land and rangeland show low Landcover area which is suspicious as a factor that causes landslide susceptible. It is also found that the fields were found on the terraces on the fragile slopes with the help of human intervention supported by landslide activation. Rest of the land use Landcover classes was shows no influence on landslide occurrences.

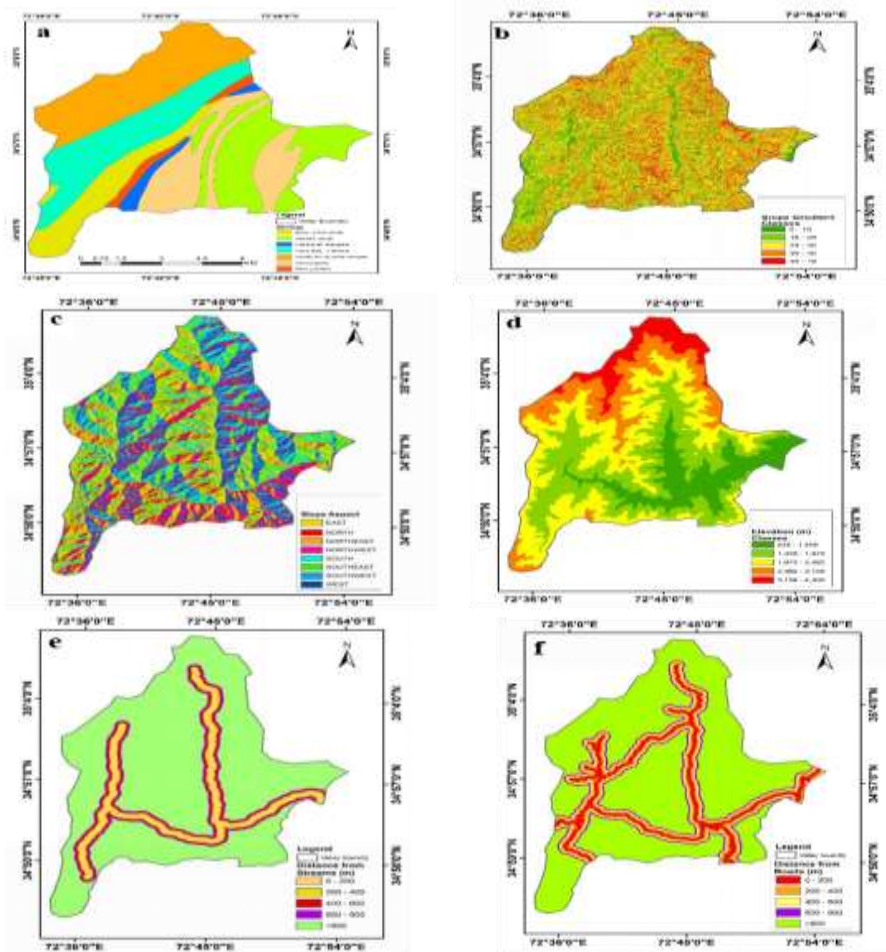
3.2.16 Distance from fault and relative effect model

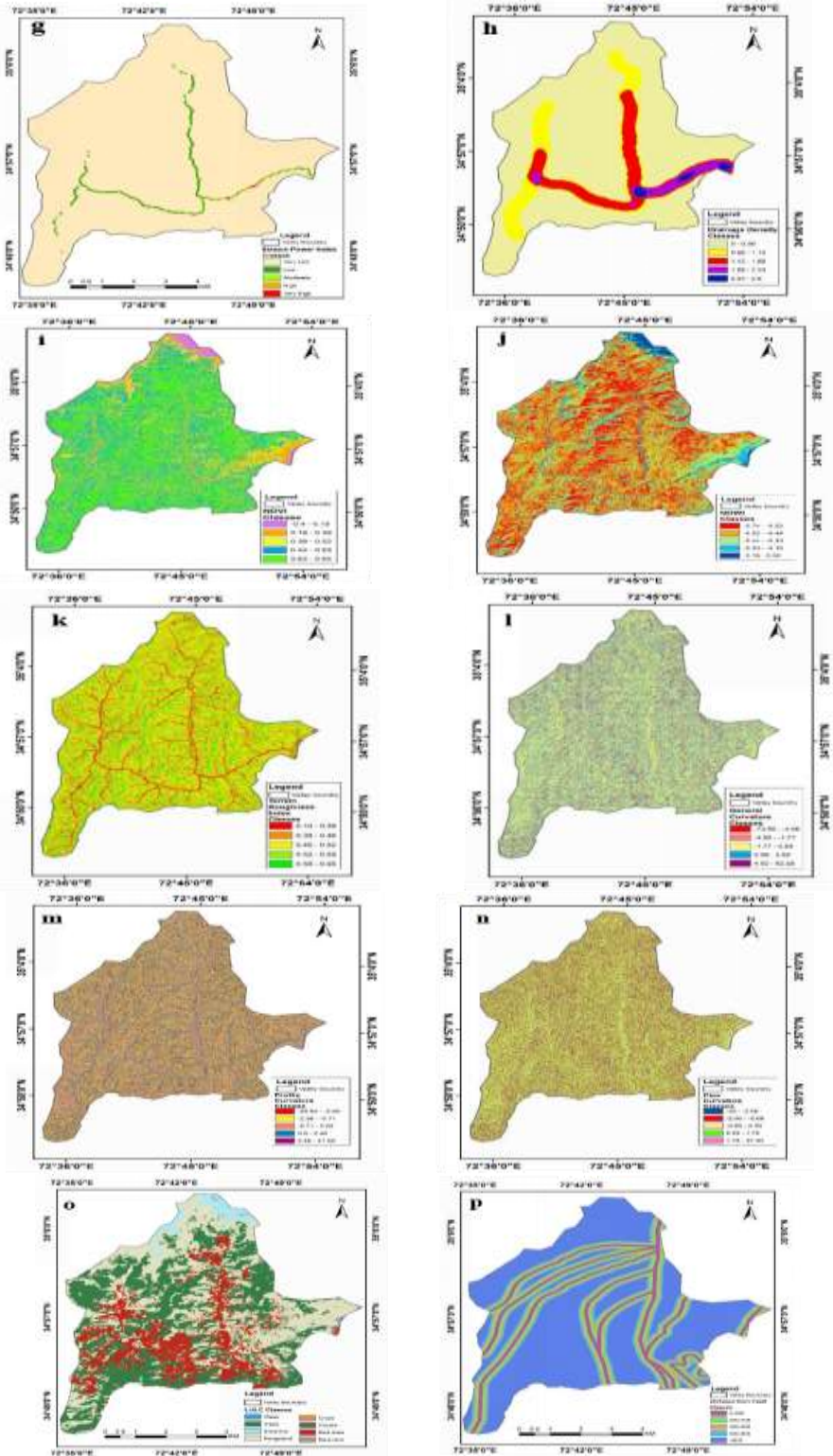
Active and deep fault structure controls the landslide's development. Fault map of the study area was digitized from the geologic map of the Beshani and Allai-Kohistan areas (Baig, 1990). Distance from fault was determined by multiple buffer technique with 200m intervals and classified into five buffer zones as shown in Fig 3p. The purpose of the buffers was to determine the proximity to each fault line on landsliding. Relative effect values were determined by using the relative effect model. the analysis shows that the buffer class 0 to 400 is showing positive values of 0.172 and 0.105, respectively. They show a high possibility of landslides due to reducing the cohesion power of rock and a strong correlation with landslide occurrences. The results show that an area near the fault line has high possibility and is more susceptible to landslide than the area further away (Fig 4p; Table 1). The analysis of Rehman et al. (2019) also showed that the landslide susceptibility score was high near to fault line and decreased when moving away from the faultlines.

3.2.17 Rainfall and relative effect model

Extent And Evaluation of Landslide Probability, Triggering Factors and Model Validation in Sub-Humid and Seismically Active Area of District Shangla, Eastern Hindukush

Rainfall is the triggering factor for landslide occurrence (Bordoni et al., 2015; Abdo, 2021). It is considered a geo-environmental factor. Long-term excessive rainfall causes landslides in the study area. It decreases the shear strength of the material, opens the pores of the soil/rock mass and creates flow conditions resulting in landslides. It also supported the erosion process and surface runoff. The Global precipitation measurement mission (GPM) data was used for rainfall mapping. the interpolation technique such as Inverse Distance weightage was used to prepare the rainfall map of the study area (Fig 3q). In Fig 4q; Table 1, the analysis revealed that rainfall from 96.73mm to 105.67mm is indicating the positive relative effect values of 0.22 and 0.11 respectively and showing the strong relationship between the landslides and causative factor (Table 1) and thus highly prone to landslide events.





Extent And Evaluation of Landslide Probability, Triggering Factors and Model Validation in Sub-Humid and Seismically Active Area of District Shangla, Eastern Hindukush

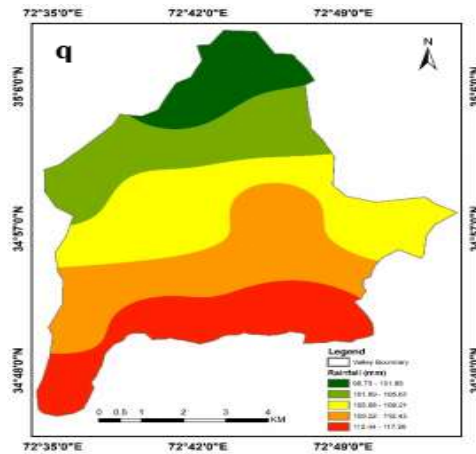
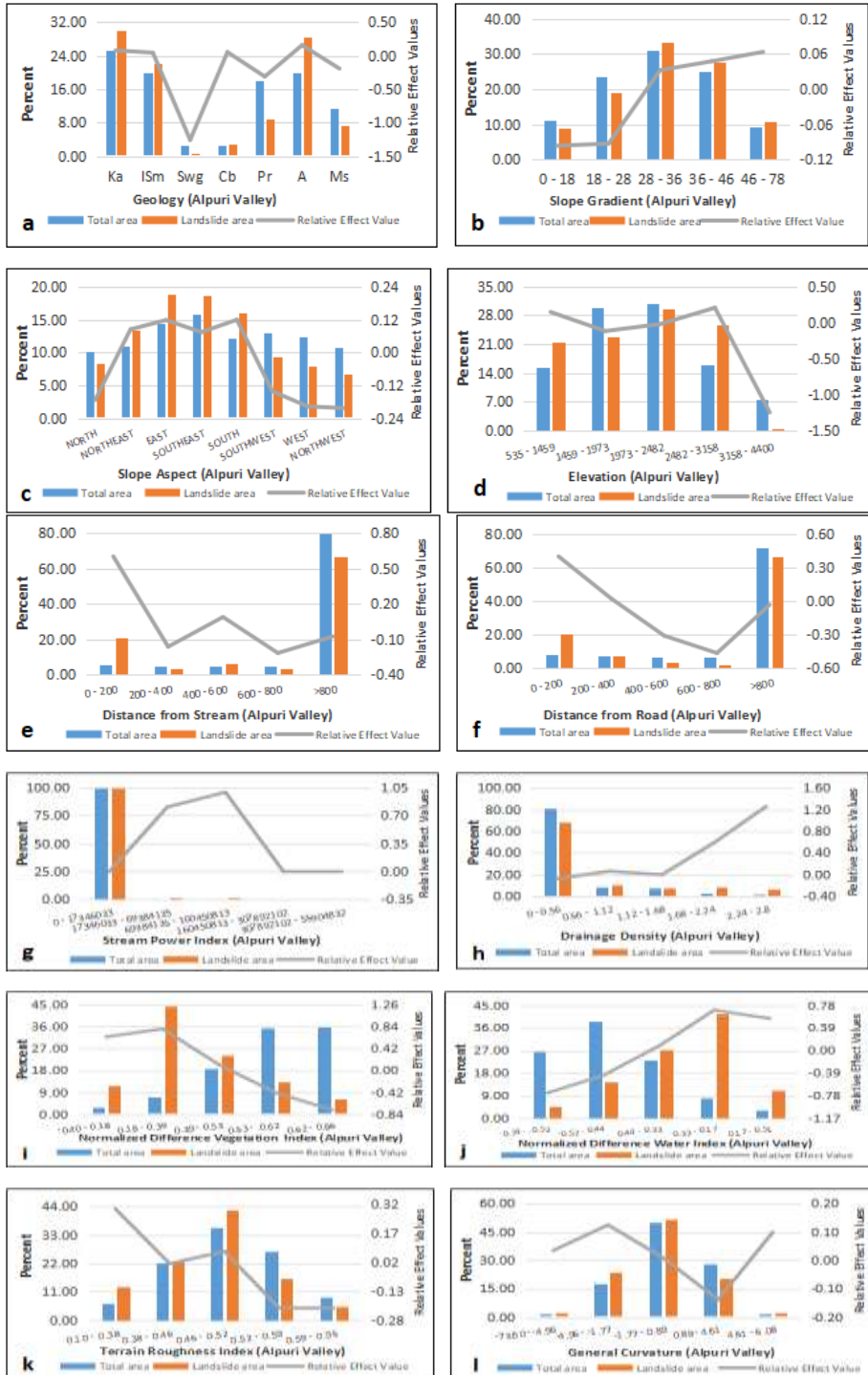


Fig. 3 Thematic maps of the study area: (a) geology; (b) slope gradient; (c) slope aspect; (d) elevation; (e) distance from river; (f) distance to road; (g) stream power index; (h) drainage density; (i) NDVI; (j) NDWI; (k) TRI; (l) general curvature; (m) profile curvature; (n) plan curvature; (o) LULC; (p) Distance from fault lines; (q) Rainfall

In this study, 17 causative factors were used to prepare the landslide susceptibility map of the study area. Relative effect values of each class of 17 causative factors were computed and show their impact on landsliding. Overall results revealed that the slope with gentle to steep having the northeast to southward slope facing, having the geology units of Besham formation, Kamila Amphibolite complex, Indus Suture melange and Cambriam Manglaur with the elevation of 535 to 3158 m and buffer zones 0 to 200m and 400 to 600m of distance from stream, buffer zones of 0 to 400m of distance from roads and faults show high possibility of landslide occurrences. Landuse Landcover with Bare land and Rangeland classes with high intensive rainfall in monsoon season, with high density of water to produce high lateral erosion process where a high probability of water bodies and low and no vegetation found with low roughness area and concave like region indicated as highly susceptible to landslide events. This study suggested that this region will be further affected by recurrent landslide phenomena with climatic events. So it is very necessary to Government to take proper planning and monitoring to reduce the impact of landslides.



Extent And Evaluation of Landslide Probability, Triggering Factors and Model Validation in Sub-Humid and Seismically Active Area of District Shangla, Eastern Hindukush

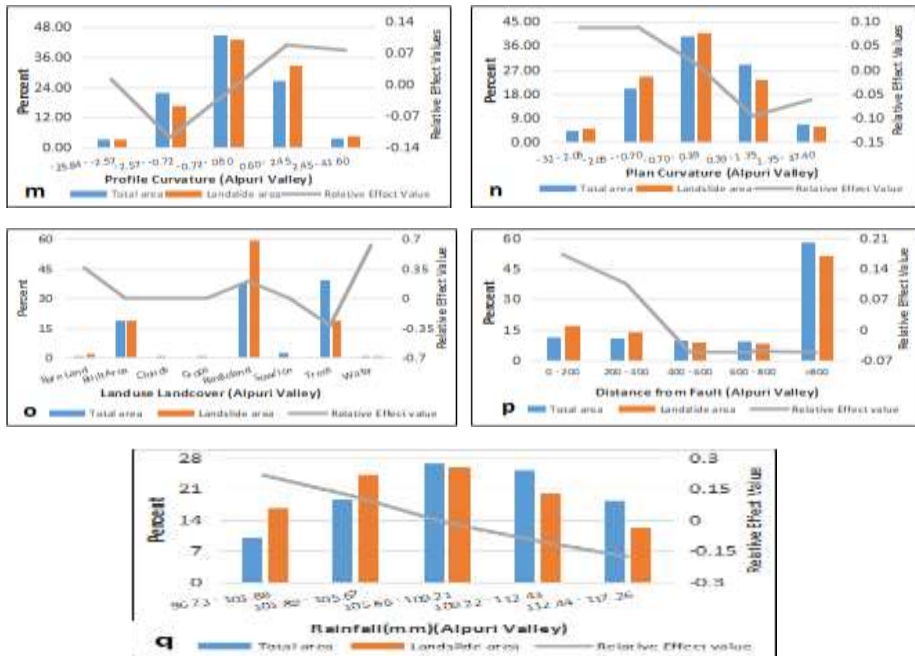


Fig. 4 percentage of landslides with the causative factors and relative effect values: (a) geology; (b) slope gradient; (c) slope aspect; (d) elevation; (e) distance from river; (f) distance to road; (g) stream power index; (h) drainage density; (i) NDVI; (j) NDWI; (k) TRI; (l) general curvature; (m) profile curvature; (n) plan curvature; (o) LULC; (p) Distance from fault; (q) Rainfall

3.3. Landslide susceptibility mapping

Landslide is one of the hazard term found in Alpuri valley which causes loss of life, destroy the human infrastructures, deforestation and loss of economy of the country. The landslide susceptibility mapping in form of zonation plays important role in planning and safety in landslide-affected areas. Preparation of landslide susceptibility map is a primary and necessary step for hazard and risk assessment. In the landslide susceptibility zonation map, the hazard areas are classified into different zones to determine the level of susceptibility on the bases of selected causative factors. All the causative factors were integrated into the GIS environment to prepare the landslide susceptibility zonation map of Alpuri valley. Landslide susceptibility map was prepared with the help of landslide susceptibility index. This index is a summation of all 17 selected factors with relative effect values which are given below:

$$LSI = \sum RE \quad (9)$$

After the preparation of the landslide susceptibility map, it was classified into four classes to identify the level of prone in Alpuri Valley as shown in Fig 5. The range of landslide susceptibility mapping was (-5.30 to 5.64). High value represented the high frequency of landslide occurrence. The classification map showed the low, moderate, high, and very high classes (Fig 5). It is analyzed that 7.55% of the susceptibility area was very high, and 25.33 % was a high susceptibility zone. Results showed that total of 32.88% area was the high landslide susceptibility zone which represented a highly prone area in future as shown in Table 2; Fig 6.

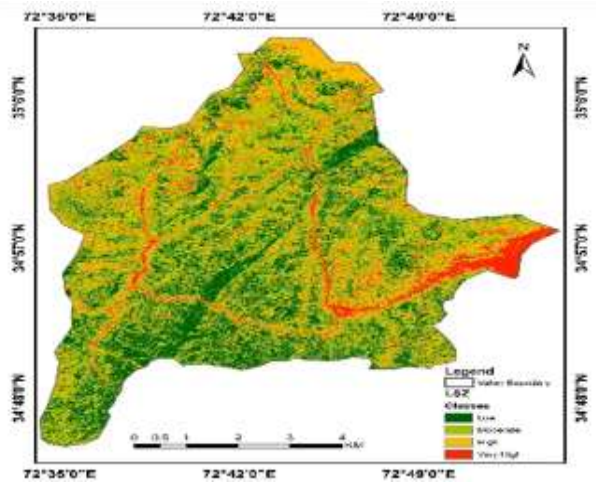


Fig. 5. Landslide susceptibility zones map of Alpuri Valley

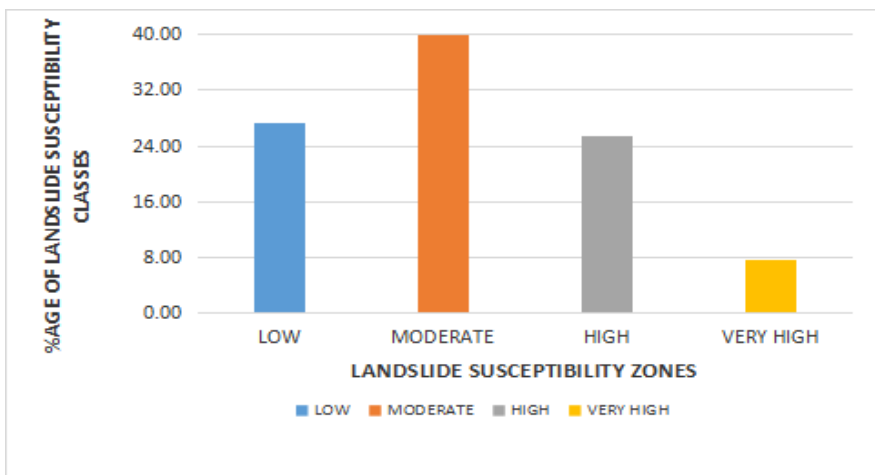


Fig. 6. Landslide Susceptibility zones of Alpuri Valley

Extent And Evaluation of Landslide Probability, Triggering Factors and Model Validation in Sub-Humid and Seismically Active Area of District Shangla, Eastern Hindukush

Table 2. Landslide susceptibility zone of Alpuri Valley

Classes	Low	Moderate	High	Very High
Alpuri				
Percentage	27.31	39.81	25.33	7.55

3.4. Validation and model performance

It is an important factor to check the validation and performance of the model in landslide susceptibility mapping. According to Chung and Fabbri (2003), it is useless and not of scientific importance without the process to check the performance and validation of models and maps. In previous studies, receiver operating characteristics (ROC) was used as a useful method for observing the performance and validation of landslide susceptibility models (Hong et al., 2017a, 2018a, b, c; Hussin et al., 2016). Area under the curve (AUC) is used for indicating the ability of the model to predict the occurrence and non-landslide occurrence pixels. Before to prepared the AUC, the past landslide inventory was divided into two data set, one is the training dataset which was used in modelling and other datasets such as testing will be used for validation purpose. Two types of curves were prepared, one is the success rate curve which is prepared by a 70% training dataset and prediction rate curve was prepared from 30% testing dataset. According to AUC values (Fig 7), the results of success rate and prediction rate curves show that the Relative model has good outcomes. AUC value and success rate curve were calculated at 0.7475 and 74.75% whereas the AUC value and prediction rate curve was calculated at 0.8787, and 87.87%. Hence, the results show that success and prediction curves fall in good citatory of AUC and satisfactory result of Relative Model identified in Alpuri Valley.

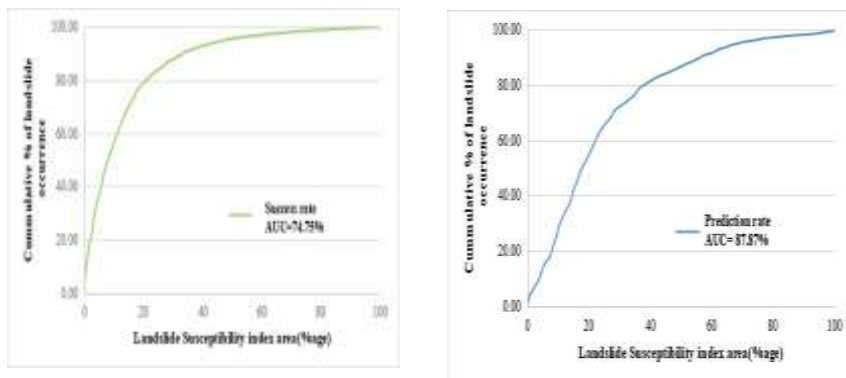


Fig. 7. Success rate and predictive rate of the landslide susceptibility map

4. CONCLUSION

In this study, Alpuri valley was selected as the landslide-prone area and find out the spatial probability of landslide occurrence. For this purpose, landslide susceptibility mapping is a very important step to determine the landslide-prone area in Alpuri valley. The main objective of this study was to utilise the Relative Effect model for preparing the landslide susceptibility map and identifying landslide probe areas. Total of 89 landslides was pointed out and digitized using GIS. 17 causative factors were selected on the availability of data in the study area. The resultant map of landslide susceptibility was prepared by combing these causative factors such as elevation, slope gradient, general curvature, slope aspect, profile curvature, plan curvature, distance from road, distance from stream, distance from faultlines, rainfall, landuse landcover, NDWI, NDVI, terrain roughness index, drainage density, stream power index and surface geology. The Relative values of every class of these factors were calculated to define the influence of landslide occurrences. The positive value of class of factors showed the high influence of landslide occurrence and negative value indicated low or no influence of landslide occurrence. The resultant landslide susceptibility map was identified into zones from low to very high. It is accounted that 7.55% and 25.33% were very high and high susceptibility zone, respectively. Total of 32.88% was considered a high susceptibility zone. Receiver operating characteristic (ROC) was used to check the validation and performance. Area under the Curve (AUC) was the area plotted under the ROC. Success rate curve and prediction rate curve accounted for the performance of model. Predictive rate curve of model was 87.87% which is used on (30%) testing data for validation purposes whereas the success rate curve was 74.75% which is used on (70%) training data for overall mapping. Accuracy of model shows the 87.87% which helps the landuse planner and decision-maker in the good planning and management.

REFERENCES

- Abdo, H. G. (2021). Assessment of landslide susceptibility zonation using frequency ratio and statistical index: a case study of Al-Fawar basin, Tartous, Syria. *International Journal of Environmental Science and Technology*, 1-20.
- Ada, M., and San, B. T. (2018). Comparison of machine-learning techniques for landslide susceptibility mapping using two-level random sampling (2LRS) in Alakir catchment area, Antalya, Turkey. *Natural hazards*, 90(1), 237-263.

Extent And Evaluation of Landslide Probability, Triggering Factors and Model Validation in Sub-Humid and Seismically Active Area of District Shangla, Eastern Hindukush

- Al-Najjar, H. A., and Pradhan, B. (2021). Spatial landslide susceptibility assessment using machine learning techniques assisted by additional data created with generative adversarial networks. *Geoscience Frontiers*, 12(2), 625-637.
- Althuwaynee, O. F., Pradhan, B., Park, H. J., and Lee, J. H. (2014). A novel ensemble bivariate statistical evidential belief function with knowledge-based analytical hierarchy process and multivariate statistical logistic regression for landslide susceptibility mapping. *Catena*, 114, 21-36.
- Arnone, E., Francipane, A., Scarbaci, A., Puglisi, C., and Noto, L. V. (2016). Effect of raster resolution and polygon-conversion algorithm on landslide susceptibility mapping. *Environmental Modelling & Software*, 84, 467-481.
- Aslam, B., Maqsoom, A., Alaloul, W. S., Musarat, M. A., Jabbar, T., and Zafar, A. (2021). Soil erosion susceptibility mapping using a GIS-based multi-criteria decision approach: Case of district Chitral, Pakistan. *Ain Shams Engineering Journal*, 12(2), 1637-1649.
- Ayalew, L., and Yamagishi, H. (2004). Slope failures in the Blue Nile basin, as seen from landscape evolution perspective. *Geomorphology*, 57(1-2), 95-116.
- Bai, S. B., Wang, J., Lü, G. N., Zhou, P. G., Hou, S. S., and Xu, S. N. (2010). GIS-based logistic regression for landslide susceptibility mapping of the Zhongxian segment in the Three Gorges area, China. *Geomorphology*, 115(1-2), 23-31.
- Baig, M. S. 1990. Structure and geochronology of Pre-Himalayan and Himalayan orogenic events in the Northwest Himalayan, Pakistan, with special reference to the Besham area published PhD thesis Department of Geology, University of Azad Jammu and Kashmir.
- Baig SU, Khan H, Muneeb F, Dad K. 2020. Formation of a hazardous ice-dammed glacier lake: a case study of anomalous behavior of Hassanabad glacier system in the Karakoram. *SN Applied Science*. 2(7), 1285.
- Bordoni M, Meisina C, Valentino R, Bittelli M, Chersich S (2015) Site-specific to local-scale shallow landslides triggering zones assessment using TRIGRS. *Natural Hazards Earth System Science*, 15(5), 1025–1050.
- Bui, D. T., Lofman, O., Revhaug, I., and Dick, O. (2011). Landslide susceptibility analysis in the Hoa Binh province of Vietnam using statistical index and logistic regression. *Natural hazards*, 59(3), 1413.

Bui, D. T., Pradhan, B., Revhaug, I., and Tran, C. T. (2014). A comparative assessment between the application of fuzzy unordered rules induction algorithm and J48 decision tree models in spatial prediction of shallow landslides at Lang Son City, Vietnam. In *Remote Sensing Applications in Environmental Research*, 87-111.

Carson. M. A, Kirkby. M. J, (1972). Hillslope form and process. Cambridge University Press, London. 475 pp.

Chen, T., Niu, R., and Jia, X. (2016). A comparison of information value and logistic regression models in landslide susceptibility mapping by using GIS. *Environmental Earth Sciences*, 75(10), 867.

Chen, X., & Chen, W. (2021). GIS-based landslide susceptibility assessment using optimized hybrid machine learning methods. *Catena*, 196, 104833.

Chung, C. J. F., and Fabbri, A. G. (2003). Validation of spatial prediction models for landslide hazard mapping. *Natural Hazards*, 30(3), 451-472.

Crozier. M. J, (1986). Landslides: causes, consequences and environment, Croom Helm. London. 252pp.

Cruden, D. M. (1991). A simple definition of a landslide. Bulletin of the International Association of Engineering Geology-Bulletin de l'Association Internationale de Géologie de l'Ingénieur, 43(1), 27-29.

Dahal, R. K., and Hasegawa, S. (2008). Representative rainfall thresholds for landslides in the Nepal Himalaya. *Geomorphology*, 100(3-4), 429-443.

Dahal, R. K., Hasegawa, S., Nonomura, A., Yamanaka, M., and Dhakal, S. (2008). DEM-based deterministic landslide hazard analysis in the Lesser Himalaya of Nepal. *Georisk*, 2(3), 161-178.

Dai, F. C., Lee, C. F., Li, J. X. Z. W., and Xu, Z. W. (2001). Assessment of landslide susceptibility on the natural terrain of Lantau Island, Hong Kong. *Environmental Geology*, 40(3), 381-391.

Dai, F. and Lee, C. (2002) Landslide characteristics and slope instability modelling using GIS, Lantau Island, Hong Kong. *Geomorphology*, 42, (3), 213-228.

Davies. T, (2015). Landslide hazards, risks, and disasters: introduction. In *Landslide Hazards, Risks and Disasters* (pp. 1-16). Academic Press.

Dikau, R. (1989). The application of a digital relief model to landform analysis in geomorphology. Three-dimensional applications in geographical information systems, 51-77.

Eker, A. M., Dikmen, M., Cambazoğlu, S., Düzgün, Ş. H., and Akgün, H. (2015). Evaluation and comparison of landslide susceptibility mapping

Extent And Evaluation of Landslide Probability, Triggering Factors and Model Validation in Sub-Humid and Seismically Active Area of District Shangla, Eastern Hindukush

methods: a case study for the Ulus district, Bartın, northern Turkey. *International Journal of Geographical Information Science*, 29(1), 132-158.

Ercanoglu, M. and Gokceoglu, C. (2002). Assessment of landslide susceptibility for a landslide-prone area (north of Yenice, NW Turkey) by fuzzy approach. *Environmental Geology*, 41(6), 720-730.

Feizizadeh, B., Blaschke, T., and Nazmfar, H. (2014). GIS-based ordered weighted averaging and Dempster–Shafer methods for landslide susceptibility mapping in the Urmia Lake Basin, Iran. *International Journal of Digital Earth*, 7(8), 688-708.

Galli, M., Ardizzone, F., Cardinali, M., Guzzetti, F., and Reichenbach, P. (2008). Comparing landslide inventory maps. *Geomorphology*, 94(3-4), 268-289.

García-Rodríguez, M. J., Malpica, J., Benito, B. and Díaz, M. (2008). Susceptibility assessment of earthquake-triggered landslides in El Salvador using logistic regression. *Geomorphology*, 95, (3), 172-191.

Ghafoori, M., Sadeghi, H., Lashkaripour, G. R., and Alimohammadi, B. (2005). Landslide hazard zonation using relative effect method: A case study in Bormahan basin, northeast Iran. *European Geosciences*, 474.

Grøneng, G., Christiansen, H. H., Nilsen, B., and Blikra, L. H. (2011). Meteorological effects on seasonal displacements of the Åknes rockslide, western Norway. *Landslides*, 8(1), 1-15.

Guo, C., Montgomery, D. R., Zhang, Y., Wang, K., and Yang, Z. (2015). Quantitative assessment of landslide susceptibility along the Xianshuihe fault zone, Tibetan Plateau, China. *Geomorphology*, 248, 93-110.

Government of Pakistan (GOP) (1987) Environmental profile of Pakistan Environment and Urban Affair Division. Government of Pakistan, Islamabad

Hong, H., Xu, C., Revhaug, I., and Bui, D. T. (2015). Spatial prediction of landslide hazard at the Yihuang area (China): a comparative study on the predictive ability of backpropagation multi-layer perceptron neural networks and radial basic function neural networks. In *Cartography-maps connecting the world*, 175-188.

Hong, H., Pradhan, B., Bui, D. T., Xu, C., Youssef, A. M., and Chen, W. (2017a). Comparison of four kernel functions used in support vector machines for landslide susceptibility mapping: a case study at Sichuan area (China). *Geomatics, Natural Hazards and Risk*, 8(2), 544-569.

Hong, H., Tsangaratos, P., Ilia, I., Liu, J., Zhu, A. X., and Chen, W. (2018a). Application of fuzzy weight of evidence and data mining techniques in construction of flood susceptibility map of Poyang County, China. *Science of the total environment*, 625, 575-588.

Hong, H., Pradhan, B., Sameen, M. I., Kalantar, B., Zhu, A., and Chen, W. (2018c). Improving the accuracy of landslide susceptibility model using a novel region-partitioning approach. *Landslides*, 15(4), 753-772.

Hong, H., Panahi, M., Shirzadi, A., Ma, T., Liu, J., Zhu, A. X., and Kazakis, N. (2018b). Flood susceptibility assessment in Hengfeng area coupling adaptive neuro-fuzzy inference system with genetic algorithm and differential evolution. *Science of the Total Environment*, 621, 1124-1141.

Hussin, H. Y., Zumpano, V., Reichenbach, P., Sterlacchini, S., Micu, M., van Westen, C., and Bălteanu, D. (2016). Different landslide sampling strategies in a grid-based bi-variate statistical susceptibility model. *Geomorphology*, 253, 508-523.

Ilia, I., and Tsangaratos, P. (2016). Applying weight of evidence method and sensitivity analysis to produce a landslide susceptibility map. *Landslides*, 13(2), 379-397.

Iqbal, J., Cui, P. E. N. G., Hussain, M. L., Pourghasemi, H. R., & Pradhan, B. (2021). Landslide susceptibility assessment along the dubair-dud ishal section of the Karakoram highway, northwestern Himalayas, Pakistan. *Acta Geodynamic Geomater*, 18(2), 137-155.

Jaafari, A., Najafi, A., Pourghasemi, H. R., Rezaeian, J., and Sattarian, A. (2014). GIS-based frequency ratio and index of entropy models for landslide susceptibility assessment in the Caspian forest, northern Iran. *International Journal of Environmental Science and Technology*, 11(4), 909-926.

Jebur, M. N., Pradhan, B., and Tehrany, M. S. (2014). Manifestation of LiDAR-derived parameters in the spatial prediction of landslides using novel ensemble evidential belief functions and support vector machine models in GIS. *IEEE Journal of Selected Topics in Applied Earth Observations and Remote Sensing*, 8(2), 674-690.

Jehan, N., and Ahmad, I. (2006). Petrochemistry of asbestos bearing rocks from Skhakot-Qila Ultramafic Complex, northern Pakistan. *Journal of Himalayan Earth Sciences*, 39, 75-83.

Justice, C.O., Townshend, J.R.G., Holben, B.N. and Tucker, E.C.: 1985, Analysis of the phenology of global vegetation using meteorological satellite data. *International Journal of Remote Sensing*, 6, 1271-1318.

Extent And Evaluation of Landslide Probability, Triggering Factors and Model Validation in Sub-Humid and Seismically Active Area of District Shangla, Eastern Hindukush

- Kamp, U., Owen, L. A., Growley, B. J., and Khattak, G. A. (2010). Back analysis of landslide susceptibility zonation mapping for the 2005 Kashmir earthquake: an assessment of the reliability of susceptibility zoning maps. *Natural hazards*, 54(1), 1-25.
- Kannan M, Saranathan E, Anabalagan R (2013) Landslide vulnerability mapping using frequency ratio model: a geospatial approach in Bodi-Bodimettu Ghat section, Theni district, Tamil Nadu, India. *Arabian Journal of Geosciences*, 6(8):2901–2913
- Kepr, B. (1969) Differential geometry. In: Rektorys, K. (Ed.), Survey of Applicable Mathematics. M.I.T. Press, Cambridge, pp. 298–372.
- Khan, M.S., Ashraf, M., and Chaudry, M.N. (1997) Geochemical evidence for the tectonic setting of the Punjal volcanic in Azad Kashmir and Kaghan valley areas. *Geol. Bull. Univ. Punjab*, 31-32.
- Khan, A. N. (2000). Landslide hazard and policy response in Pakistan: a case study of Murree, Pakistan. *Science Vision*, 6(1), 35-48.
- Khan H, Shafique M, Khan MA, et al. (2019) Landslide susceptibility assessment using Frequency Ratio, a case study of northern Pakistan. *Egypt Journal of Remote Sensing and Space Science*, 22(1): 11-24.
- Khan, M. B. A., Rahman, A. U., and Shaw, R. (2022). Integration of Socioeconomic Dynamics and Communities' Resilience to Landslides in Swat Valley, Pakistan. In *Impact of Climate Change, Land Use and Land Cover, and Socio-economic Dynamics on Landslides*, 335-370.
- Khattak, G. A., Owen, L. A., Kamp, U., and Harp, E. L. (2010). Evolution of earthquake-triggered landslides in the Kashmir Himalaya, northern Pakistan. *Geomorphology*, 115(1-2), 102-108.
- Kouli, M., Loupasakis, C., Soupios, P., and Vallianatos, F. (2010). Landslide hazard zonation in high-risk areas of Rethymno prefecture, Crete Island, Greece. *Natural Hazards*, 52(3) 599– 621.
- Lee, S., and Min, K. (2001). Statistical analysis of landslide susceptibility at Yongin, Korea. *Environmental Geology*, 40(9), 1095-1113.
- Lee, S., and Talib, J. A. (2005). Probabilistic landslide susceptibility and factor effect analysis. *Environmental Geology*, 47(7), 982-990.
- Lundgren, L. (1978). Studies of soil and vegetation development on fresh landslide scars in the Mgeta Valley, Western Uluguru Mountains, Tanzania. *Geografiska Annaler: Series A, Physical Geography*, 60(3-4), 91-127.

- Luo, W., and Liu, C. C. (2018). Innovative landslide susceptibility mapping supported by geomorphic and geographical detector methods. *Landslides*, 15(3), 465-474.
- Lv, L., Chen, T., Dou, J., and Plaza, A. (2022). A hybrid ensemble-based deep-learning framework for landslide susceptibility mapping. *International Journal of Applied Earth Observation and Geoinformation*, 108, 102713.
- McFeeters, S. K. (1996). The use of the Normalized Difference Water Index (NDWI) in the delineation of open water features. *International journal of remote sensing*, 17(7), 1425-1432.
- Meena SR, Gudiyangada Nachappa T (2019) Impact of spatial resolution of digital elevation model on landslide susceptibility mapping: a case study in Kullu Valley, Himalayas. *Geosciences*, 9, 360.
- Mitra, D., Bhandery, C., Mukhopadhyay, A., Chanda, A., and Hazra, S. (2018). Landslide risk assessment in Darjeeling hills using multi-criteria decision support system: a Bayesian network approach. In *Disaster Risk Governance in India and Cross-Cutting*, 361-386.
- Mohammady M, Pourghasemi HR, Pradhan B (2012) Landslide susceptibility mapping at Golestan Province, Iran: a comparison between frequency ratio, Dempster-Shafer, and weights of-evidence models. *Journal of Asian Earth Sciences*, 61:221–236
- Mondal, S., and Mandal, S. (2018). RS & GIS-based landslide susceptibility mapping of the Balason River basin, Darjeeling Himalaya, using logistic regression (LR) model. *Georisk: Assessment and Management of Risk for Engineered Systems and Geohazards*, 12(1), 29-44.
- Moore, I. D., Grayson, R. B., and Ladson, A. R. (1991). Digital terrain modelling: a review of hydrological, geomorphological, and biological applications. *Hydrological processes*, 5(1), 3-30.
- Moore, I. D., and Wilson, J. P. (1992). Length-slope factors for the Revised Universal Soil Loss Equation: Simplified method of estimation. *Journal of soil and water conservation*, 47(5), 423-428.
- Moore, I.D., Lewis, A., and Gallant, J.C. (1993b). Terrain attributes estimation methods and scale effects. In: Jakeman, A.J., Beck, M.B., McAleer, M.J. (Eds.). *Modelling Change in Environmental Systems*. 189–214.
- Moore, I. D., Gessler, P. E., Nielsen, G. A. E., and Peterson, G. A. (1993a). Soil attribute prediction using terrain analysis. *Soil science society of America Journal*, 57(2), 443-452.

Extent And Evaluation of Landslide Probability, Triggering Factors and Model Validation in Sub-Humid and Seismically Active Area of District Shangla, Eastern Hindukush

Myronidis, D., Papageorgiou, C., and Theophanous, S. (2016). Landslide susceptibility mapping based on landslide history and analytic hierarchy process (AHP). *Natural Hazards*, 81(1), 245-263.

Naveen Raj, T.; Ram Mohan, V.; Backiaraj, S.; Muthusamy, S. (2011) Landslide hazard zonation using the relative effect method in the southeastern part of Nilgiris, Tamil Nadu, India. *International Journal of Engineering Science and Technology*, 3, (4), 3260–3266.

Neelakantan, R.; Yuvaraj, S. Relative effect-based landslide hazard zonation mapping in parts of Nilgiris, Tamil Nadu, South India. *Arabian Journal of Geosciences*, 2013, 6(11), 4207-4213

Nefeslioglu, H. A., Duman, T. Y., and Durmaz, S. (2008). Landslide susceptibility mapping for a part of tectonic Kelkit Valley (Eastern Black Sea region of Turkey). *Geomorphology*, 94(3-4), 401-418.

Nefeslioglu, H., Gokceoglu, C., and Sonmez, H. (2008). An assessment of the use of logistic regression and artificial neural networks with different sampling strategies for the preparation of landslide susceptibility maps. *Engineering Geology*, 97, (3), 171-191.

Pareek, N., Sharma, M. L., and Arora, M. K. (2010). Impact of seismic factors on landslide susceptibility zonation: a case study in part of Indian Himalayas. *Landslides*, 7(2), 191-201.

Pham, B. T., Prakash, I., and Bui, D. T. (2018). Spatial prediction of landslides using a hybrid machine learning approach based on random subspace and classification and regression trees. *Geomorphology*, 303, 256-270.

Pham, B. T., Bui, D. T., Dholakia, M. B., Prakash, I., Pham, H. V., Mehmood, K., and Le, H. Q. (2017a). A novel ensemble classifier of rotation forest and Naïve Bayer for landslide susceptibility assessment at the Luc Yen district, Yen Bai Province (Viet Nam) using GIS. *Geomatics, Natural Hazards and Risk*, 8(2), 649-671.

Pham, B. T., Bui, D. T., Pourghasemi, H. R., Indra, P., and Dholakia, M. B. (2017b). Landslide susceptibility assessment in the Uttarakhand area (India) using GIS: a comparison study of prediction capability of naïve Bayes, multilayer perceptron neural networks, and functional tree methods. *Theoretical and Applied Climatology*, 128(1-2), 255-273.

Pourghasemi, H. R., Pradhan, B., and Gokceoglu, C. (2012). Application of fuzzy logic and analytical hierarchy process (AHP) to landslide susceptibility mapping at Haraz watershed, Iran. *Natural hazards*, 63(2), 965-996.

- Pourghasemi, H.R., Timoori Yansari, Z., Panagos, P. and Pradhan, B. (2018). Analysis and evaluation of landslide susceptibility: A review on articles published during 2005-2016 (periods of 2005-2012 and 2013- 2016). *Arabian Journal of Geosciences*, 11, 193.
- Pradhan, A. M. S.; Kim, Y. T. (2014). Relative effect method of landslide susceptibility zonation in weathered granite soil: a case study in Deokjeok-ri Creek, South Korea. *Natural hazards*, 72(2), 1189-1217.
- Rahman A., and R. Shaw (2015). Floods in the Hindu Kush region: Causes and socio-economic aspects. In: *Mountain Hazards and Disaster Risk Reduction*, 33-52.
- Rahman, G., Rahman, A., Samiullah, and Collins, A. (2017) Geospatial analysis of landslide susceptibility and zonation in Shahpur valley, Eastern Hindu Kush using frequency ratio model; *Proc. Pakistan Academy. Sci.* 54(3) 149–163.
- Rahman, G., Rahman, A. U., Anwar, M. M., Dawood, M., & Miandad, M. (2022). Spatio-temporal analysis of climatic variability, trend detection, and drought assessment in Khyber Pakhtunkhwa, Pakistan. *Arabian Journal of Geosciences*, 15(1), 1-13.
- Ramesh, V.; Anbazhagan, S.(2015) Landslide susceptibility mapping along Kolli hills Ghat road section (India) using frequency ratio, relative effect and fuzzy logic models. *Environmental Earth Sciences*, 73(12), 8009-8021.
- Razavizadeh, S, Solaimani, K, Massironi, M, et al. (2017) Mapping landslide susceptibility with frequency ratio, statistical index, and weights of evidence models: a case study in northern Iran. *Environmental Earth Sciences*, 76(14), 499.
- Rehman, A., Song, J., Haq, F., Mahmood, S., Ahamad, M. I., Basharat, M., ... and Mehmood, M. S. (2022). Multi-Hazard Susceptibility Assessment Using the Analytical Hierarchy Process and Frequency Ratio Techniques in the Northwest Himalayas, Pakistan. *Remote Sensing*, 14(3), 554.
- Reichenbach, P., Galli, M., Cardinali, M., Guzzetti, F., and Ardizzone, F. (2005). Geomorphologic mapping to assess landslide risk: concepts, methods and applications in the Umbria Region of central Italy. *Landslide Risk Assessment*, 429-468.
- Restrepo, C., Vitousek, P., Neville, P. (2003). Landslides significantly alter land cover and the distribution of biomass: an example from the Ninole ridges of Hawai'i. *Plant Ecology*, 166(1), 131–143.
- Sezer, E. A., Nefeslioglu, H. A., and Osna, T. (2017). An expert-based landslide susceptibility mapping (LSM) module developed for Netcad Architect Software. *Computers & Geosciences*, 98, 26-37.

Extent And Evaluation of Landslide Probability, Triggering Factors and Model Validation in Sub-Humid and Seismically Active Area of District Shangla, Eastern Hindukush

- Riley, S. J., DeGloria, S. D., and Elliot, R. (1999). Index that quantifies topographic heterogeneity. *Intermountain Journal of Sciences*, 5(1-4), 23-27.
- Shirzadi, A.; Bui, D.T.; Pham, B.T.; Solaimani, K.; Chapi, K.; Kavian, A.; Shahabi, H.; Revhaug, I. (2017). Shallow landslide susceptibility assessment using a novel hybrid intelligence approach. *Environmental Earth Science*, 76, 60.
- Shit, P. K., Bhunia, G. S., and Maiti, R. (2016). Potential landslide susceptibility mapping using weighted overlay model (WOM). *Modeling Earth Systems and Environment*, 2(1), 21.
- Sun X, Chen J, Bao Y, Han X, Zhan J, Peng W. (2018) Landslide susceptibility mapping using logistic regression analysis along the Jinsha River and its tributaries close to Derong and Deqin County, Southwestern China. *ISPRS International Journal of Geo-Informatics*, 7(11):438.
- Thomas Jr., G.B. (1968) *Calculus and Analytic Geometry: Part Two Vectors and Functions of Several Variables*. Addison-Wesley Publishing, Reading, MA, USA. 784 pp.
- Udin, W. S., Yahaya, N. N. and Shariffuddin, S. I. M. (2021). Landslide susceptibility assessment using geographic information system in Aring, Gua Musang, Kelantan. In IOP Conference Series: *Earth and Environmental Science*, 842(1), 012008.
- UNDP (2006) Disaster risk reduction workshop by BEGIN-ER UNDP for Line Departments of District Shangla April 16-18, 2006.
- Vandromme, R., Thiery, Y., Bernardie, S., & Sedan, O. (2020). ALICE (Assessment of Landslides Induced by Climatic Events): A single tool to integrate shallow and deep landslides for susceptibility and hazard assessment. *Geomorphology*, 367, 107307.
- Wang Q, Li W (2017) A GIS-based comparative evaluation of analytical hierarchy process and `Hasher area, Jizan (Saudi Arabia) using GIS-based frequency ratio and index of entropy models. *Geosciences Journal*, 19(1), 113-134.
- Zaz, S. N., & Romshoo, S. A. (2022). Landslide susceptibility assessment of Kashmir Himalaya, India. *Arabian Journal of Geosciences*, 15(6), 1-18.
- Zhao, C., Chen, W., Wang, Q., Wu, Y., and Yang, B. (2015). A comparative study of statistical index and certainty factor models in landslide susceptibility mapping: a case study for the Changzhou District, Shaanxi Province, China. *Arabian Journal of Geosciences*, 8(11), 9079-9088.